Journal of Materials Science Research and Reviews

3(1): 1-13, 2019; Article no.JMSRR.47105

Study on Electrical, Optical Properties of $ZnSe/SiO_2$ Composite Thin Film Using Sol-Gel Dip Coating Techniques

Mohana Faroug Attia[1*]

[1]*Department of Mechanical Engineering - Physics, Alasala Colleges Alahlia, College of Engineering, Dammam, P.O.Box 2666, Dammam, 31483, Saudi Arabia.*

Author's contribution

The sole author designed, analysed, interpreted and prepared the manuscript.

Article Information

Editor(s):
(1) Dr. Serkan Islak, Associate Professor, Department of Metallurgical and Materials Engineering, Faculty of Engineering and Architecture, Kastamonu University, Turkey.
Reviewers:
(1) Rana Abdul Shakoor, Qatar University, Qatar.
(2) Yuan-Tsung Chen, National Yunlin University of Science and Technology, Taiwan, R.O.C.
(3) Manal Abd El Moneim Mahdy, National Research Centre, Egypt.
Complete Peer review History: http://www.sdiarticle3.com/review-history/47105

Original Research Article

Received 07 November 2018
Accepted 14 February 2019
Published 14 March 2019

ABSTRACT

This study seeks to obtain data about electric and optical properties of $ZnSe/SiO_2$ composite films for Photovoltaic Applications, for this purpose ZnSe nanoparticles established in [Si O_2] thin films were prepared by sol-gel method using zinc acetate dihydrate [Zn $(CH_3\ COO)_2\ .2H_2O$], selenic acid [H_2SeO_4] and Tetraethyl orthosilicate [$Si(OC_2H_5)_4$]. The n – ZnSe /SiO_2 thin film composites were deposited on the glass substrate by dip coating technique. Mobility activation has been studied from the photocurrent degradation curves. XRD results indicate the phase structure of ZnSe particles embedded in $ZnSe/SiO_2$ composite thin films is sphalerite (cubic ZnS). The effective density of states (N_{eff}), frequency factor (S), and trap depth (E) have been calculated for all the films having different crystallite sizes. The increase in photoconductivity is explained in terms of built in potential barriers (φ_b) at the crystallite boundaries. Field Emission Scanning Electron Microscopy (FESEM) image show that morphology of n - ZnSe influenced by $ZnSe/SiO_2$ molar ratio. The optical characterization of thin film composite has been examined by transmittance measurement in the UV-visible wavelength range. It was found that the optical transmission is decreased with increase of the $ZnSe/SiO_2$ molar ratio. The highest transmission of 54.6% and the

**Corresponding author: Email: mohana.attia@alasala.edu.sa;*

lowest of 36.7% were acquired for the specimens with 5% and 20% $ZnSe/SiO_2$ molar ratio, respectively. Further observation shows that the optical transition in $ZnSe/SiO_2$ thin film is direct transition with band gap energy in the range of 2.6 - 3.9 eV.

Keywords: Electrical properties; optical properties; sol-gel; $ZnSe/SiO_2$; morphology; thin film.

1. INTRODUCTION

In recent years, nanocrystalline materials are being researched widely because of their electronic and optical characteristic depend on their size. As one of the broad band gaps II-VI semiconducting material widely applied in optoelectronic devices, owing to its bandgap (2.7 eV) belongs to the visible region [1-5]. ZnSe is a highly photosensitive semiconductor, so nanocrystalline ZnSe can be synthesized by many methods such as pulsed laser deposition [6], chemical vapor deposition [7], molecular beam epitaxy, and sol-gel method [8,9]. ZnSe is also attractive host for the formation of doped nanocrystal [10]. In thin film form, ZnSe and Cu-doped nanoparticle multilayer composite films have been prepared by Hao et al. [11]. Recently, a novel oleic acid-controlled hydrothermal route was applied to produce ZnSe quantum dots in stable solution [12]. In addition to improved mechanical and electrical properties, the transition from bulk material to nanoparticles is expected to yield an increased dominance of surface atoms and thus enhancement of the material's chemical reactivity [13]. Another special characteristic associated with nanoparticles is the controllability of their electrical conductivity through external manipulation (voltage, flux, absorption and emission of photons), making them suitable for many kinds of electrical and optical applications [14]. Selenides, which are very useful materials, have been widely used as thermoelectric cooling materials, optical filters, optical recording materials, solar cells, supersonic materials, and sensor and laser materials [15]. The sol - gel method is one of the most popular method since its simple and a cheap method. In this study, sol - gel dip coating was found play function an outstanding role as a soft bottom- up approach to achieve nano - sized ZnSe in oxide thin films.

2. METHODOLOGY

ZnSe nanoparticles in SiO_2 thin films were prepared by sol-gel dip coating technique. The sol of SiO_2 was firstly prepared from Tetraethyl orthosilicate mixed with deionized water under ammonium hydroxide as catalyst. Then, acetic acid was added into the solution to set pH of the solution. After that, zinc acetate dihydrate and selenic acid were then added to the solution as zinc and selenium sources, respectively. The thin films were deposited on the glass substrate using dip coating method at room temperature, followed by annealed under argon atmosphere at 500°C for 1 hour to obtain the ZnSe nanoparticles/SiO_2 thin film composites.

2.1 Materials Characterization

The phase structure of $ZnSe/SiO_2$ thin films was investigated by XRD (Rigaku D/MAX-2400, Cu Kα). The relationship of ellipsometric angle with wavelength of ZnSe/SiO2 thin composite film was investigated through spectroscopic ellipsometers (M-2000U1, J.A. WOOLAM. Co. Inc). The field emission scanning electron microscopy (FESEM) equipped with EDX spectrometer (Zeiss SUPRA 35VP) was used for determination of microstructure and elemental composition of films. The optical properties of thin films have been investigated via transmittance measurement using UV-Vis. Spectrophotometer (Labomed – UVS 2800) in the wavelength range of 200 nm – 1100 nm. A Filmetric UV20 was used to determine the film thickness.

3. RESULTS AND DISCUSSION

Since the films were prepared with variation of the molar ratio of $ZnSe/SiO_2$ (from 5% to 20%), it was found that the thickness of the films increase with the increasing of $ZnSe/SiO_2$ molar ratio. The viscosity of the precursors affected by molarities may explain the increasing of film thickness. Viscosity of the sol will tend to increase with the increasing of the molar ratio of $ZnSe/SiO_2$ because the size of ZnSe crystals contributed to increasing the overall film thickness. The result also indicates that the thickness increases significantly when the molar ratio of $ZnSe/SiO_2$ has been going up to 20 %. This may be the cause of the orientation of the ZnSe dot in the SiO_2 matrix. When the molar ratio of $ZnSe/SiO_2$ increased, a larger number of ZnSe dots will embed in the oxide layer.

Therefore, the distance between the dots became shorter in the deposited films.

3.1 The XRD Analysis

The XRD of ZnSe/SiO_2 thin films synthesized at 500°C shown in Fig. 1. The XRD pattern indicated that the structure of ZnSe is sphalerite (cubic ZnS) and the intensity of diffraction peak of ZnSe phase increases with the increase of reduction time. In experiment results showed that overlong time and un-sufficient heat treat time is disadvantage to prepare of ZnSe/SiO_2 thin solid films. Our further research works revealed that the reaction between selenium and oxygen at lower temperature is to occur, which means selenium element will escape seriously from the samples. At the same time, the selenium dioxide also easily decompose in relatively lower temperature. That is the reason why the over long time is disadvantage to the synthesis of ZnSe/SiO_2 thin solid films. To ensure the partial pressure of selenium element, small amounts of metal selenium also sealed in quartz tube stove. In the reduction course, oxygen must be removed as far as possible under the condition of low temperature. That is the important step to ensure ZnSe phase.

3.2 The Field Emission Scanning Electron Microscope

The (FESEM) images of the samples SiO_2 and ZnSe/SiO_2 thin film composite shown in Fig.1. Smooth surface structure was observed in pure SiO_2 samples as shown in Fig 2 (a) However, when ZnSe introduced to SiO_2 host material, the varied size and structures of ZnSe nanoparticles were found embedded in SiO_2 and confirmed the formation of ZnSe/SiO_2 thin film composites as shown in Fig. 2(b – f) At lower ZnSe/SiO_2 molar ratio of 5%, only a little amount of ZnSe particles appear in host material of SiO_2 films (Fig. 2(b)) Significant amount of ZnSe nanoparticles were found in the sample with 10% or more ratio. From image, we can see that small size of spherical shape nanoparticles was randomly distributed inside and surface of the host films (Fig. 2 (c)) When molar ratio of ZnSe/SiO_2 increases to 15%, there are many nanoparticles have embedded in SiO_2 film and some of them form nanocluster structures. Further increasing in molar ratio to 20%; produce the agglomerated structures as shown in Fig. 2(e). The EDX analysis results on the pure SiO_2 thin film and ZnSe/SiO_2 thin films composite are shown in Fig. 3 From EDX result obtained that the only Si and O elements detected in the host material of pure silica films (Fig. 3(a)) However, EDX analysis on a selected composite sample (5 % molar ratio) shows the existence of Zn and Se elements (Fig. 3(b)) This result may indicate the formation of ZnSe compound embedded in the SiO_2 host film. Meanwhile, the presence of calcium (Ca) element in this sample is come from glass substrate. The EDX analysis data for SiO_2 thin films shown in Table 1. The EDX analysis data for ZnSe nanoparticles embedded in SiO_2 thin films presented in Table 2.

From EDX result obtained that the only Si and O elements detected in the host material of pure silica films (Fig. 2(a)) However, EDX analysis on a selected composite sample (5% molar ratio) shows the existence of Zn and Se elements (Fig. 3 (b)) This result may indicate the formation of ZnSe compound embedded in the SiO_2 host film. Meanwhile, the presence of calcium (Ca) element in this sample is coming from glass substrate.

3.3 Electrical Properties

As photocurrent (I_{ph}) rises to a steady state value and a peak is observed in rise curves of SnSe films. In materials, having traps in the mobility gap, the recombination time of carriers is same as carrier life time when free carrier density is more than trapped carrier density [16]. The trap depth (*E*) in nanocrystalline ZnSe/SiO_2 thin films has been calculated using the relation [17],

$$E = \left[\ln s - ln\left\{\frac{\ln\left(\frac{t_0}{t_t}\right)}{t}\right\}\right] \quad (1)$$

Table 1. EDX analysis data for SiO_2 thin films

Element	Wt. %	At. %
O K	58.72	68.73
Si K	41.28	31.27

Table 2. EDX analysis data for ZnSe nanoparticles embedded in SiO_2 thin films

Element	Wt. %	At. %
O K	48.59	64.56
Zn L	6.05	1.99
Se L	1.14	0.53
Si K	43.20	32.30
Ca K	1.01	0.61

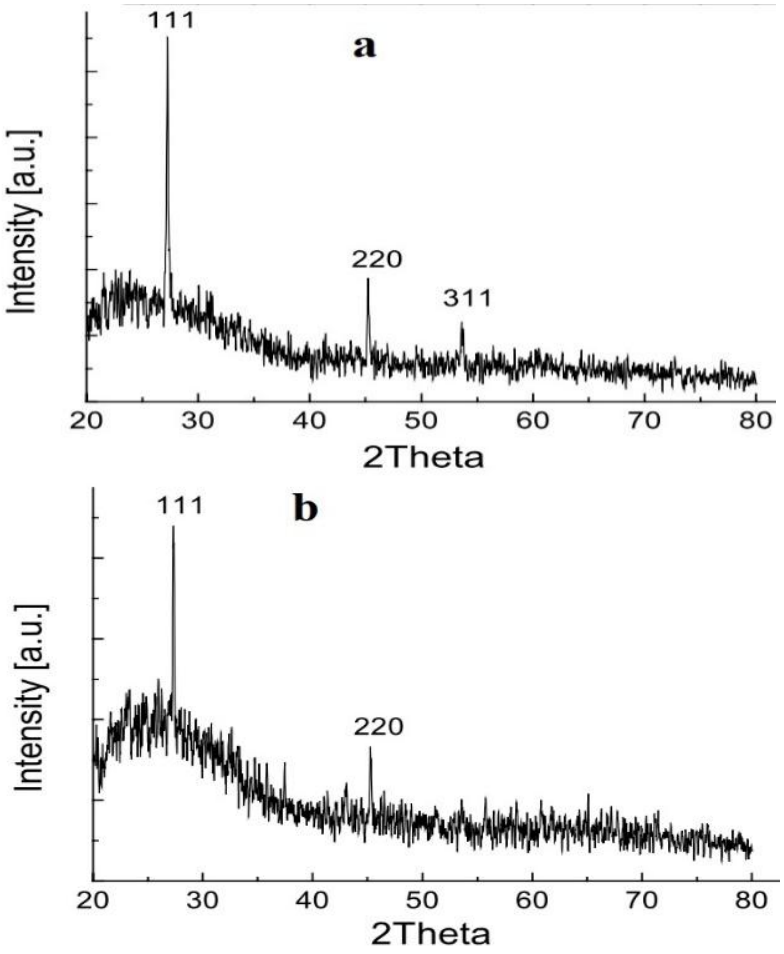

Fig. 1. The XRD patterns of $ZnSe/SiO_2$ composite thin films (synthesized at 500 ^{0}C)

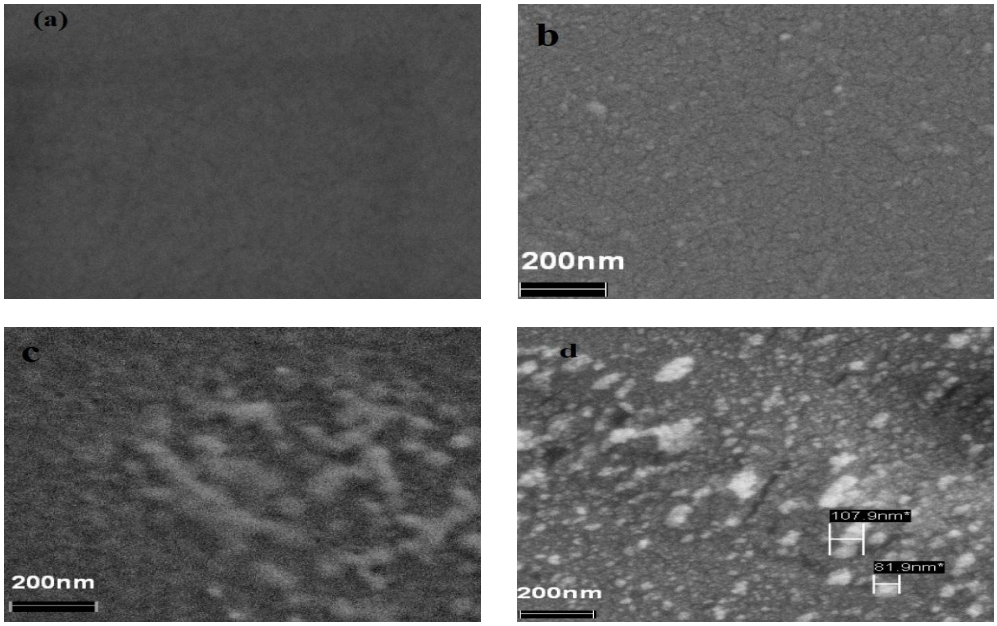

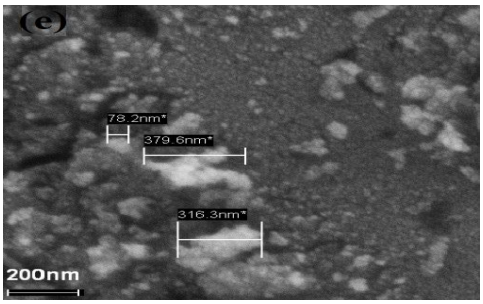

Fig. 2. FESEM images of the samples (a) pure SiO_2 thin films (b) 5 % (c) 10 % (d) 15 % (e) 20 % wt. of $ZnSe/SiO_2$

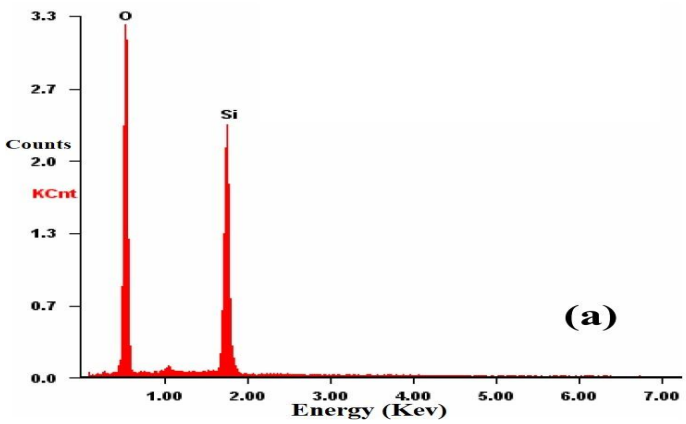

Fig. 3a. EDX analysis results on the (a) pure SiO_2 thin films

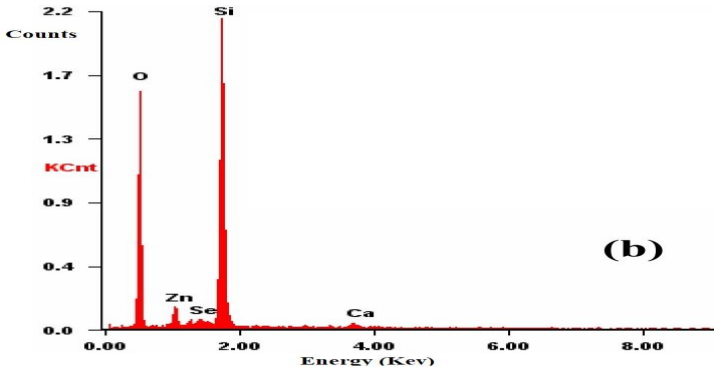

Fig. 3b. EDX analysis results on the (b) ZnSe nanoparticles embedded in SiO_2 thin films (5% molar ratio)

where I_0 is the photocurrent when the illumination is stopped, I_t is the photocurrent at any subsequent time, t, after the termination of illumination, and S is the frequency factor [18]. The frequency factor can be calculated using;

$$S = N_{eff}\, \upsilon_{th}\, St \qquad (2)$$

where N_{eff} is the effective density of states in the conduction band, v_{th} is the thermal velocity, and S_t is the capture cross section of electrons.

N_{eff} is calculated by conductivity data with an assumption that the number of occupied energy levels in the conduction band is identical as $N_{eff.}$

For the calculation of *S*, the values of mobility, thermal velocity, dielectric constant, and effective mass of an electron in ZnSe are considered from [19]. The calculated values of N_{eff} and *S* are represented in Table 3. The crystallite grain size of the ZnSe/SiO_2 thin film was calculated using the Scherrer's formula;

$$D = \frac{k\lambda}{\beta \cos\theta} \quad (3)$$

Where *k* is about 0.94 and β is the Full Width at Half Maximum (FWHM).

The trap depths for these films are calculated using the slopes of ln (I_0 / It) vs. time plots and S. The different values of trap depths are also systematically presented in Table 3. One part of the photo-generated carriers recombines with respective opposite charges localized at grain boundary depletion regions, thereby reducing the grain boundary potential barriers and the rest take part in the photoconduction process. As a result of the reduction of φ_b, the effective mobility of the carrier's increases. This process is known as barrier modulation. The decrease in φ_b also leads to increase in effective mobility, thereby increasing the conductivity of the sample. Thus, the increase in photoconductivity has two main contributors. One from the resultant increase in the photo generated carriers and the other from the increase in the effective mobility.

3.4 Effect of Annealing on ZnSe/SiO_2 Thin Films

The thin films were deposited on the glass substrate using dip coating method at room temperature, followed by annealed under argon atmosphere at 500°C for 1 hour to obtain the ZnSe/SiO_2 thin film composites.

3.5 DC Conductivity Measurements

Fig. 4 shows the temperature dependence of dark conductivity (σ_d) for the as-deposited and annealed thin films of ZnSe/SiO_2 in the temperature range 250 – 400 K. The values of σ_d for as-deposited and annealed ZnSe/SiO_2 composite films are found to be (1.76 ± 0.02) $\times 10^{-6}$ $\Omega^{-1}cm^{-1}$ and (3.11 ± 0.02) $\times 10^{-6}$ $\Omega^{-1}cm^{-1}$. Kale et al. [20] found the conductivity of the order of 10^{-7} cm^{-1}, which is in good agreement with the present results. The value of σ_d increases on annealing ZnSe/SiO_2 composite film. This increase in σ_d is due to increase in particle size on annealing [21]. The plots of *ln σd* vs. *1000/T* in Fig. 4 are straight lines in the measured temperature range which means the conduction in ZnSe/SiO_2 thin films is an activated process having single activation energy. The activation energies for *dc* conduction are calculated from the slopes of *ln* σ_d vs.*1000/T* curves and given in Table 4. The increase in electrical conductivity and activation energy after annealing may be due to the change in structural parameters, improvement in crystallite and grain size, decrease in inter-crystallite boundaries (grain boundary domains) and removal of some impurities (adsorbed and absorbed gases). Excess atoms of compound are also possible [22] due to a small change in stoichiometry after annealing.

3.6 Steady State Photoconductivity

Fig. 5 shows the temperature dependence of photoconductivity for as deposited and annealed ZnSe thin films. The values of photoconductivity are calculated to (8.67±0.02) × 10^{-6} Ω^{-1} cm^{-1}, and (1.19±0.02) × 10^{-5} Ω^{-1} cm^{-1} for as deposited and annealed thin films. The photo activation energies ($\Delta\varepsilon_{ph}$) are calculated using the slopes of curve shown in Fig. 5. The activation energies for photoconduction are much smaller than for the dark conduction. The value of σ_{ph} increases with the annealing. No maximum in the steady state photoconductivity with temperature has been observed in the measured temperature range. Photosensitivity is found to increase after annealing.

3.7 Transient Photoconductivity

Fig. 6 shows the rise and decay curves of I_{ph} for as deposited and annealed ZnSe/SiO_2 thin films. As I_{ph} rises to a steady state value and a peak is observed in rise curves of ZnSe/SiO_2 composite films. During decay, the photocurrent does not reach zero for a long time after the incident light is switched off. A persistent photocurrent is observed in both the cases. This type of photoconductive decay has also been reported in various other semiconductors [23-25]. The decay of I_{ph} is slow for all ZnSe/SiO_2 composite film.

The values of decay constant (τ_d) at different times have been calculated using Equation;

$$\tau_d = -\left[\frac{1}{I_{ph}} \frac{d\, I_{ph}}{dt}\right]^{-1} \quad (4)$$

for as deposited and annealed ZnSe/SiO_2 thin films from the slopes (at different times) of decay curves of Fig. 6. The value of τ_d as given in Table 4 increases with time which indicates

that the traps are present at all the energies in the band gap of all samples. These traps have different time constants and hence giving the non-exponential decay of photoconductivity. Fig. 6 shows the plots of $ln\ \tau_d$ vs. *ln t* for all samples at intensity 8450 lux. The extrapolation of the curves at t = 0, give the values of the carrier life time and are found to be, 2.16 and 2.23 seconds for as deposited and annealed films respectively. Clearly, the carrier life time increases on annealing the film. The straight lines in Fig. 7, obey a power law of the form t^{-N}, with $N = d(ln\ \tau_d\ /ln\ t)$ and the values of *N* are found to be 0.362 and 0.418 for as-deposited and annealed ZnSe thin films respectively.

3.8 Current Voltage (I-V) Characteristics

I-V graph of as-deposited time varying ZnSe thin films prepared is shown in Fig. 8. During I-V measurement, the supply voltage was 0-20 Volts. From the Figs. 8 and 10, it is observed that the I-V graph shows the ohmic nature of $ZnSe/SiO_2$ thin films [26]. From Figs. 8 and 9, it is observed that the I-V slop of the time varying $ZnSe/SiO_2$ film are almost similar.

Table 3. Some electrical parameters for $ZnSe/SiO_2$ thin films with different crystallite grain sizes

Grain size (nm)	N_{eff} (cm^{-3})	S (s^{-1})	E_1 (eV)	E_2 (Ev)	E_3 (Ev)
22.2	6.68×10^{11}	1.68×10^{7}	0.48	0.47	0.46
18.5	1.79×10^{9}	4.50×10^{4}	0.27	0.26	0.25
06.7	1.17×10^{10}	2.96×10^{5}	0.32	0.31	0.30

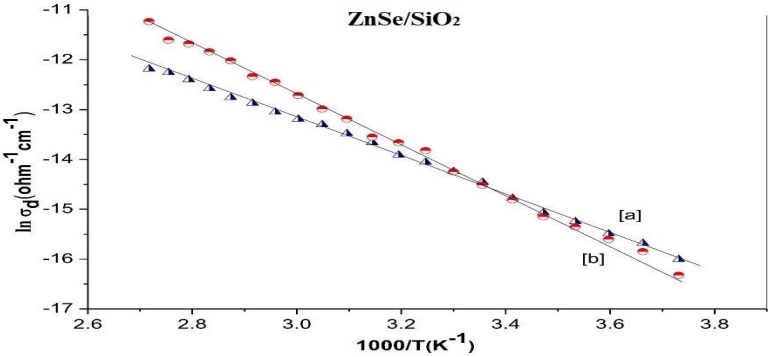

Fig. 4. Plot of ln σ_d vs. 1000/T of [a] as-deposited [b] annealed $ZnSe/SiO_2$ thin films

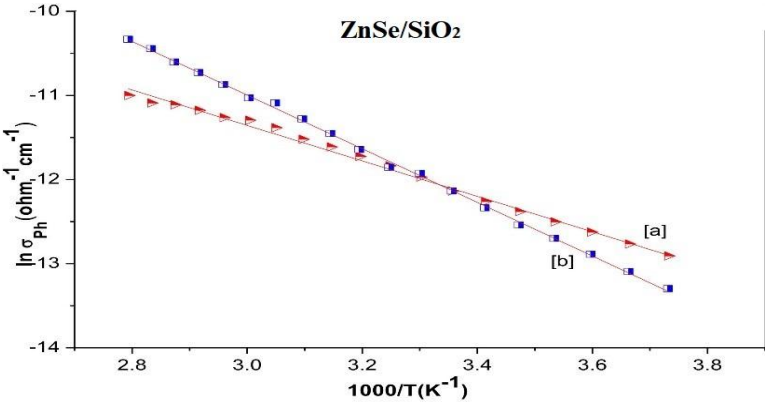

Fig. 5. Plot of ln σ_{ph} vs. 1000/T of [a] as-deposited and [b] annealed $ZnSe/SiO_2$ thin films

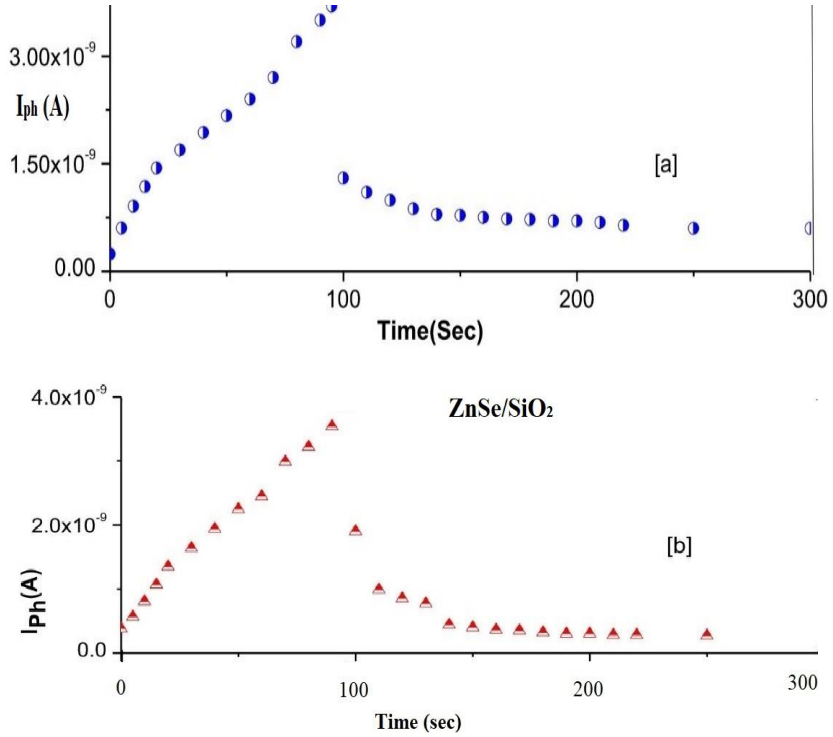

Fig. 6. The rise and decay curves of I_{ph} for [a] as-deposited and [b] annealed $ZnSe/SiO_2$ thin films

Table 4. List of various electrical parameters for as deposited and annealed $ZnSe/SiO_2$ thin films

$ZnSe/SiO_2$ thin films	σ_d (Ω^{-1} cm^{-1})	$\Delta\varepsilon_d$ (eV)	σ_{ph} (Ω^{-1} cm^{-1})	$\Delta\varepsilon_{ph}$ (eV)	σ_{ph} / σ_d	$\ln\tau_{d(t=0)}$ (sec)
As-deposited	1.76×10^{-6}	0.75	8.67×10^{-6}	0.41	4.92	2.163
Annealed	3.11×10^{-6}	0.97	1.19×10^{-5}	0.63	3.84	3.84

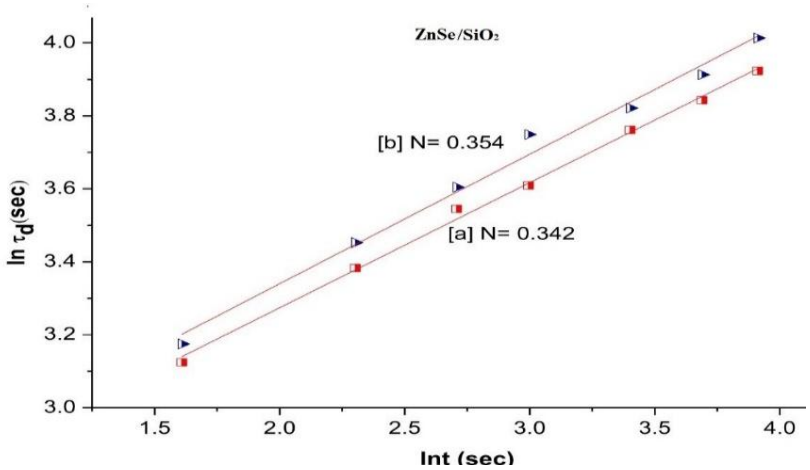

Fig. 7. Plot of ln τ_d vs. ln t for [a] as-deposited and [b] annealed $ZnSe/SiO_2$ thin films

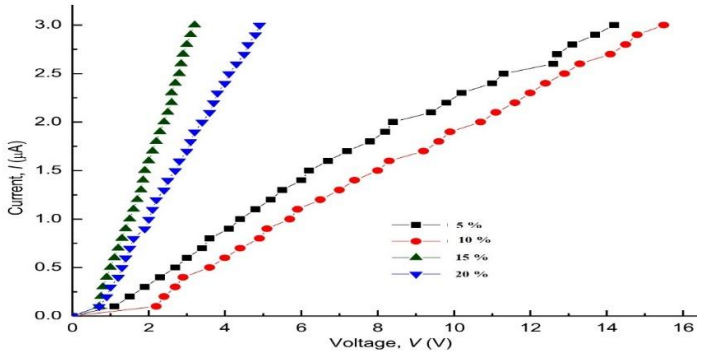

Fig. 8. I-V characteristics graph of as-deposited ZnSe/SiO_2 thin films

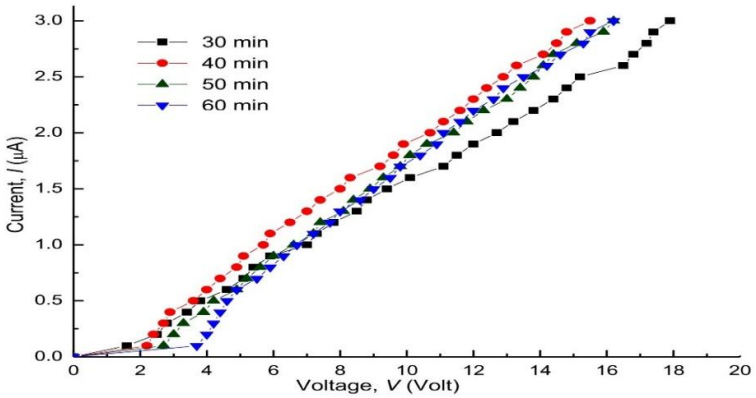

Fig. 9. I-V characteristic graph of as-deposited ZnSe/SiO_2 thin film

3.9 Optical Properties

The optical properties of thin films have been investigated via transmittance measurement using UV-Vis. Spectrophotometer (Labomed – UVS 2800) in the wavelength range of 200 nm – 1100 nm. The results show that the transmission of thin films is decreases when increase the molar ratio of ZnSe/SiO_2 as shown in Fig. 9(a). It may be caused by the thickness of film composite which was found lightly increases from 125.9 nm (5% molar ratio) to 135.5 nm (20% molar ratio) with increment of molar ratio. In Fig. 9(a), the highest transmittance of film composite is 54.6% for 5% ZnSe/SiO_2 molar ratio. The lowest transmittance value of 36.7% was obtained for the sample with 20% ZnSe/SiO_2 molar ratio. Transmittance values of other samples are lies in between the two samples. This high transmission value is in line with the fact that ZnSe is a semiconductor material with large band gap energy. For comparison, in Fig. 9(a) also shows the transmission spectra for empty glass substrate as the highest among them which is up to 87.4%. The curves also show that optical absorption edges are slightly blue-shifted at different molar ratio. Interestingly, we can see from the curves, the strong absorption peaks are lies at about 275 nm wavelength for several films with different molar ratios of ZnSe/SiO_2.

The optical absorption coefficient, α was calculated using well known relation;

$$\alpha = \frac{1}{d} \ln\left[\frac{1}{T}\right] \quad (5)$$

The absorption coefficient was calculated by processing the recorded optical spectra of thin film composites according to equation 5. The explored spectral range is region of intrinsic absorption [26]. In this spectral range the electronic transitions from valence band to conduction band produce free charge carriers. Fig. 9(b) shows graph of absorption coefficient against photon energy at different molar ratios. The absorption coefficient for ZnSe/SiO_2 thin film composites lies in the range of 6 x10^4 to 1.3x10^5 cm^{-1} for the photon energies range of 2.0

– 4.5 eV. The curve shows that absorption coefficient is increases with photon energy. There are at least three strong absorption peaks have been detected in the curves with absorption coefficient values of 132013, 118380 and 93529 cm^{-1} corresponding to the samples prepared by $ZnSe/SiO_2$ molar ratio of 12 %, 10% and 15%, respectively (Fig. 9(b)). However, the samples prepared of 5% and 20 % $ZnSe/SiO_2$ molar ratio show the flat curve of absorption coefficient which were saturated at 81187 and 79682 cm^{-1}, respectively.

Type of optical transition can be determined using the following equations [27]. For indirect transition is:

$$\alpha h\nu = A(h\nu - E_g \pm E_p)^r \quad (6)$$

where α is absorption coefficient, *Eg* is energy gap, *A* is a constant, *h* is Planck constant, v is photon frequency and *Ep* is phonon energy, either absorbed (+) or emitted (-). Theoretically r = 2 for indirect allowed transition and r = 3 for indirect forbidden transition.

The optical energy gap was determined from the absorption spectra of direct allowed transition:

$$(\alpha h\nu)^2 = A(h\nu - E_g) \quad (7)$$

Fig. 10 shows graph $(\alpha h\nu)^2$ versus photon energy *(hv)* for samples prepared at different molar ratio of $ZnSe/SiO_2$. By extrapolation of linear portion of $(\alpha h\nu)^2$ versus *hv* curves obtained the band gap energy of 3.7, 3.8, and 3.9 eV for samples with $ZnSe/SiO_2$ molar ratio of 15 %, 12%, and 10 %, respectively. However, lower band gap energy values of 2.6 and 2.7 eV obtained for the samples 20 % and 5 % molar ratio, respectively. The band gap energies for the samples prepared by 10 %, 12 % and 15 % $ZnSe/SiO_2$ molar ratio are much higher if compared to the band gap energy value of ZnSe bulk material, which is about 2.7 eV at room temperature [28]. These band gap value of the three samples also higher than $ZnSe/SiO_2$ thin films prepared by chemical bath deposition (which is 2.9 eV) [29, 30] and in a good agreement with those reported by Jun et al. [31] for zinc selenide quantum dots prepared via a temperature controlled molecular precursor approach. The blue shift of band gap energy at room temperature is due to the confinement effects. In other words, the ZnSe crystals behave as quantum dots or have three dimensionally confined structures. Even though, the band gap energy of the samples prepared by 5 % and 20 % $ZnSe/SiO_2$ molar ratio are very close to bulk material value. This phenomenon may be due to increases the size of ZnSe dots at higher $ZnSe/SiO_2$ molar ratio (20 %) and SiO_2 play role in lower molar ratio (5 %). The high $ZnSe/SiO_2$ molar ratio (20 %) may also cause the poor crystallization of ZnSe dots and distributed randomly in the film. Changing the geometry of the surface of the quantum dot also changes the band gap energy, owing to the small size of the dot, and the effects of quantum confinement. Size of the band gap is controlled by the size of the dot. More shifts from bulk value will occur with the decrease in the size of quantum dots. Because the 20 % $ZnSe/SiO_2$ thin film contains the quantum dots in bigger size, so the band gap energy is near to bulk material with just a little energy shifts from the bulk condition.

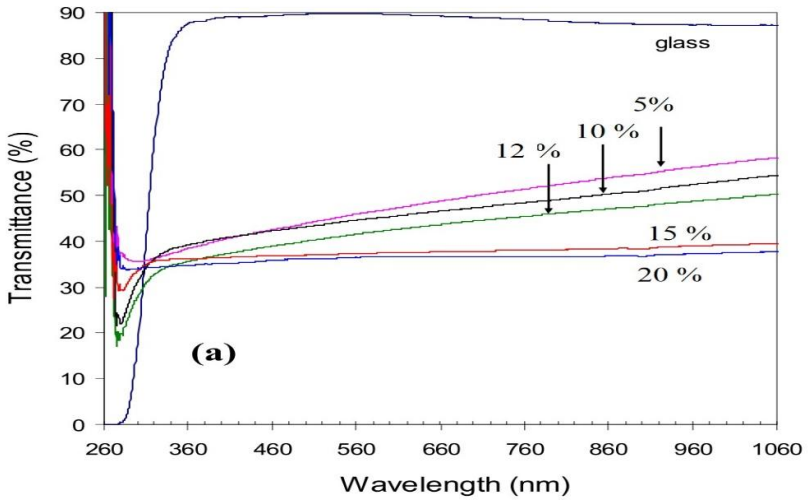

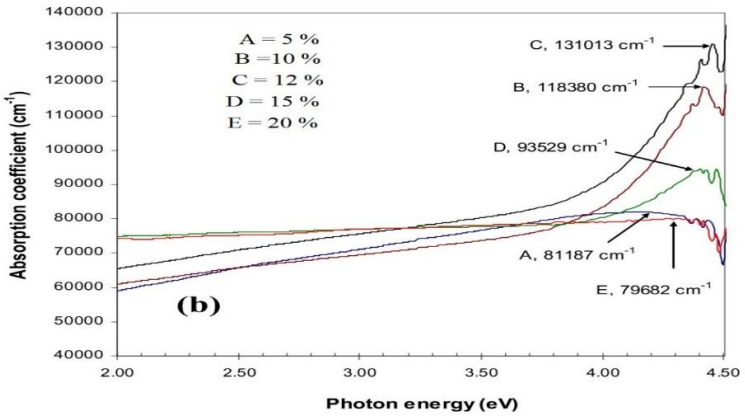

Fig. 9. (a) Transmission versus wavelength, and (b) absorption coefficient against photon energy of different ZnSe/SiO_2 molar ratios

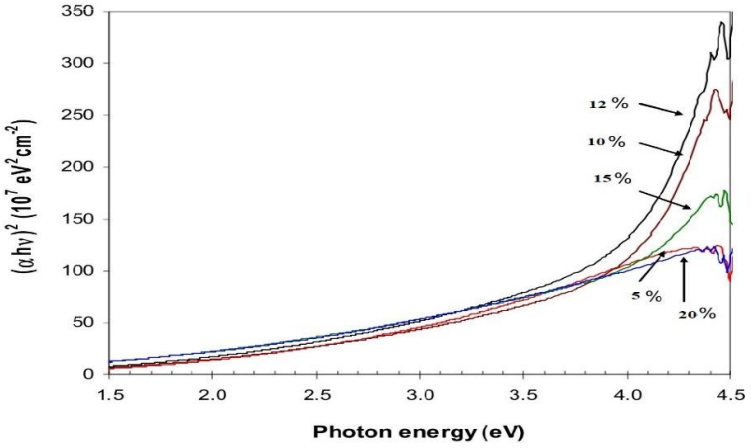

Fig. 10. $(\alpha h\nu)^2$ versus photon energy (hν) for samples prepared at different molar ratio of ZnSe/SiO_2

4. CONCLUSIONS

In the present work, the optical properties of thin film composite have been investigated via transmittance measurement in the UV-Visible wavelength range. It was found that the transmittance is decreased with increase of the ZnSe/SiO_2 molar ratio. The maximum transmission is 54.6% for 5 % ZnSe/SiO_2 film and decreases to 36.7% for 20 % ZnSe/SiO_2 film, as the thickness increases from 125.9 nm to 135.5 nm. Further observation shows that the optical transition in ZnSe/SiO_2 thin film is direct transition with band gap energy in the range of 2.6 - 3.9 eV. Also, increase in the photo-generated carriers known as carrier modulation and increase of effective mobility known as barrier modulation. In the present case, trapping centers are responsible for controlling the photocurrent. Both shallow and deep traps are found to be available in these films. The observed trap depths are not single valued, and there is a quasi-continuous distribution of various traps. The conductivity of as deposited and annealed ZnSe thin films are found to be of the order of 10^{-6} - 10^{-5} cm^{-1}. The value of conductivity increases after annealing. Also, conductivity is found to be less for films having smaller particle size. The photoconductivity is found to increase with increase in particle size on annealing the film. In the measured temperature range no maximum in the steady state photoconductivity with temperature has been observed. The slope of decay curves goes on decreasing continuously as the time of decay increases. This indicates that the traps are present at all the energies in the band gap of all samples. The non-exponential decay of

photocurrent in thin films (both as-deposited and annealed) is confirmed by the increase in the value of decay time constant with increasing time.

COMPETING INTERESTS

Author has declared that no competing interests exist.

REFERENCES

1. Pejova B, Grozdanov I. Three-dimensional confinement effects in semiconducting zinc selenide quantum dots deposited in thin-film form. Mater. Chem. Phys. 2005;90:35-46. DOI:https://doi.org/10.1016/j.matchemphys.2004.08.020
2. Matasuoka T. Adv. Mater. 8, 469 (1996). DOI:https://doi.org/10.1002/adma.19960080603
3. Wang J, Hutchings DC, Miller A, et al. Laser-induced acoustic phonon gratings in semiconductor thin films. J. Appl. Phys. 1993;73:4746. DOI:https://doi.org/10.1063/1.353838
4. Hong SK, Kurts E, Chang JH, et al. Low stacking-fault density in ZnSe epilayers directly grown on epi-ready GaAs substrates without GaAs buffer layers. Appl. Phys. Lett. 2001;78:165. DOI:https://doi.org/10.1063/1.1339262
5. Jeon H, Ding J, Patterson W, et al. Blue-green injection laser diodes in (Zn, Cd)Se/ZnSe quantum wells. Appl. Phys. Lett. 1991;59:3619. Available:https://doi.org/10.1063/1.105625
6. Li G, Nogami M. Preparation and optical properties of sol-gel derived ZnS crystallites doped in glass films. J. Appl. Phys. 1994;75:4276-4278. DOI:https://10.1063/1.355970.
7. Rao CNR, Vivekchand SRC, Biswas K, Govindaraj A. Synthesis of inorganic nanomaterials. Dalton Trans. 2007;34: 3728. DOI:https://10.1039/B708342D
8. Leppert VJ, Mahamuni S, Kumbhojkar NR, Risbud SH. Structural and optical characteristics of ZnSe nanocrystals synthesized in the presence of a polymer capping agent. Mater. Sci. Eng. B. 1998;52:89-92. DOI:https://doi.org/10.1016/S0921-5107(97)00142-6
9. Jiang H, Yao X, Che J, Wang M, Kong F. Preparation of ZnSe quantum dots embedded in SiO_2 thin films by sol-gel process. Ceram. International. 2004;30: 1685-1689. DOI:https://doi.org/10.1016/j.ceramint.2004.03.030
10. Norris DJ, Yao N, Charnock FT, Kennedy TA. High-quality manganese-doped ZnSe nanocrystals. Nano Lett. 2001;1(3). DOI:https://10.1021/nl005503h
11. Hao E, Zhang H, Yang B, Ren H, Shen J. Preparation of luminescent polyelectrolyte/ Cu-doped ZnSe nanoparticle multilayer composite films. J. Colloids Interf. Sci. 2001;238:285-290. DOI:https://doi.org/10.1006/jcis.2001.7472
12. Jiao Y, Yu D, Wang Z, Tang K, Sun X. Synthesis, nonlinear optical properties and photoluminesce of ZnSe quantum dots in stable solution. Mater. Lett. 2007;61:1541-1543. DOI:https://doi.org/10.1016/j.matlet.2006.07.103
13. Chen W, Zhang JZ, Joly AG. Optical properties and potential applications of doped semiconductor nanoparticles. J Nanosci Nanotechnol. 2004;4:919-947. DOI:https://doi.org/10.1166/jnn.2004.142
14. Singhi V, Verma N. Effect of heat treatment on ZnS: Eu Nanoparticles: synthesis and characterization; 2009. Available:http://tudr.thapar.edu:8080/jspui/bitstream/10266/826/3/826.pdf.
15. Junjie Zhu, Yuri Koltypin, Gedanken A. General sonochemical method for the preparation of nanophasic selenides: Synthesis of ZnSe nanoparticles. Chem. Mater. 2000;12(1):73–78. DOI:https://10.1021/cm990380r
16. Harbeke G. (Ed.). Polycrystalline semiconductors: Physical properties and applications. Springer, Berlin; 1984. ISBN 978-3-642-82441-8
17. Sharma J, Tripathi SK. Effect of deposition pressure on structural, optical and electrical properties of zinc selenide thin films. Physica B. 2011;406:1757-1762. DOI:https://doi.org/10.1016/j.physb.2011.02.022
18. Bube RH Photoconductivity of solids. Wiley, New York (1960). ASIN: B0000CKOL8
19. Singh J. Physics of semiconductors and their heterostructures. McGraw-Hill, New York; 1993. ISBN-13: 978-0070576070
20. Kale RB, Lokhande CD. Band gap shift, structural characterization and phase transformation of Cd Se thin films from

nanocrystalline cubic to nanorod hexagonal on air annealing. Semicond. Sci. Technol. 2005;20:1-9. DOI:https://10.1088/0268-1242/20/1/001
21. Rattanachan ST, Krongarrom P, Fangsuwannarak T. Influence of annealing temperature on characteristics of bismuth doped zinc oxide film. American Journal of Applied Sciences. 2013;10(11):1427-1438. DOI:https://10.3844/ajassp.2013.1427.1438
22. Rusu GI, Popa ME, Rusu GG, Salaoru I. On the electronic transport properties of polycrystalline ZnSe films. Appl. Surf. Sci. 2003;218:223-231. DOI:https://doi.org/10.1016/S0169-4332(03)00618-4
23. Harbeke G. (Ed.). Polycrystalline semiconductors: Physical properties and applications. Springer, Berlin. ISBN 978-3-642-82441-8; 1984.
24. Harbeke G. (Ed.). Polycrystalline semiconductors: Physical properties and applications. Springer, Berlin. ISBN 978-3-642-82441-8; 1984
25. Sharma J, Shikha D, Tripathi SK. Electrical characterization of nanocrystalline zinc selenide thin films. Journal of Theoretical and Applied Physics. 2012;6:(16):1-5. DOI:https://10.1186/2251-7235-6-16
26. Pejova B, Tanusevski A, Grozdanov I. Semiconducting thin films of zinc selenide quantum dots. J. Sol. Stat. Chem. 2004;177:4785-4799. DOI:https://10.1016/j.jssc.2004.06.011
27. Wahab Y, Hutagalung SD, Sakrani S. Optical absorption in tin selenide thin films. SPIE. 1998;3175:295-301. DOI:https://10.1117/12.300689
28. Grebe G, Roussos G, Schulz HJ. Cr^{2+} excitation levels in ZnSe and ZnS. J. Phys. C: Sol. Stat. Phys. 1976;9:4511-4516. DOI:https://10.1088/0022-3719/9/24/020
29. Lokhande CD, Patil PS, Tributsch H, Ennaoui A. ZnSe thin films by chemical bath deposition method. Solar Energy Mater. Solar Cells. 1998;55:379-393. DOI:https://doi.org/10.1016/S0927-0248(98)00112-3
30. Lokhande CD, Patil PS, Ennaoui A, Tributsch H. Chemical bath ZnSe thin films: Deposition and characterization," App. Surf. Sci. 1998;123/124:294-297. DOI:https://doi.org/10.1016/S0169-4332(97)00520-5
31. Jun YW, Koo JE, Cheon J. One-step synthesis of size tuned zinc selenide quantum dots via a temperature controlled molecular precursor approach. Chem. Commun. 2000;14:1243-124. DOI:https://10.1039/B002983L

Peer-review history:
The peer review history for this paper can be accessed here:
http://www.sdiarticle3.com/review-history/47105